Sulfur Isotope Anomalies (Δ 33 S) in Urban Air Pollution Linked to Mineral-Dust-Associated Sulfate

Sanjeev Dasari, Guillaume Paris, Bruna Saar, Qiaomin Pei, Zhiyuan Cong, David Widory

SO_2 photo-oxidation on mineral dust: The missing link to explain $\Delta^{33}S$ anomalies in urban sulfate aerosols

Sanjeev Dasari[1*], Guillaume Paris[2], Bruna Saar[3], Qiaomin Pei[4],
Zhiyuan Cong[4], David Widory[3*]

[1]Institut des Géosciences de l'Environnement (IGE), Université Grenoble Alpes, CNRS, IRD, Grenoble INP, Grenoble 38000, France

[2]Université de Lorraine, CRPG, CNRS, Vandœuvre-lès-Nancy 54500, France

[3]GEOTOP/ Université du Québec à Montréal, Montréal H3C 3P8, Canada

[4]Key Laboratory of Tibetan Environment Changes and Land Surface Processes, Institute of Tibetan Plateau Research, Chinese Academy of Sciences, Beijing 100101, China

KEYWORDS

Sulfur Mass-Independent Fractionation (S-MIF), UV radiation, Air Pollution, Particulate Matter, Model-Observation Reconciliation

ABSTRACT

Sulfate aerosols exert a net cooling effect on the earth-atmosphere system, yet their radiative forcing remains associated with largest of uncertainties in the assessment of climate change. One of the contributing factors is the poor understanding of the sulfate formation pathways, which are thought to be following mostly the mass-dependent fractionation model (i.e., $\Delta^{33}S \sim 0$). However, globally, urban sulfate aerosols exhibit significant non-zero $\Delta^{33}S$ compositions (from -0.6‰ to +0.6‰), resulting in sulfur mass-independent fractionation (S-MIF) processes. The origin(s) of these S-MIF anomalies remain(s) unclear. Here, we conducted dual-isotope ($\Delta^{33}S$, $\delta^{34}S$) probing of sulfate aerosols from summertime megacity Delhi in South Asia. A shift towards concomitantly high $\Delta^{33}S$ (from +0.2‰ to +0.5‰) and low $\delta^{34}S$ (from +5‰ to +1‰) values was observed with the influx of mineral dust. The Fe-to-Al tracer showed significant correlations with sulfate loadings (R^2=0.84) and $\Delta^{33}S$ signatures (R^2=0.77). As such, we postulate that the SO_2 photo-oxidation on mineral dust generates S-MIF anomaly ~ +0.35±0.10‰, thereby also explaining the previously observed $\Delta^{33}S$ values worldwide. Together, the findings help deconvolute S-isotope dynamics in urban regions wherein, contrary to prevailing paradigm, non-anthropogenic factor (i.e., mineral dust) is found to influence the aerosol sulfate-induced pollution affecting air quality/human health.

SYNOPSIS

Sulfate-related pollution in urban regions—affecting air quality/human health—could be linked to non-anthropogenic factor i.e., mineral dust.

INTRODUCTION

Sulfur (S) is one of the essential elements for life. The sulfur biogeochemical cycle contributes to controlling the redox state of Earth's surface and links the atmosphere, biosphere, hydrosphere, and the lithosphere[1]. Yet, the sulfur cycle is massively disrupted by human activities[1-3]. The majority of natural and anthropogenic S is released directly as SO_2 (gas) or oxidized into SO_2 in the atmosphere[2]. On a global scale, ~50% of SO_2 (natural and anthropogenically emitted) is oxidized to sulfate while the rest is lost to dry and wet scavenging[3]. The pathway taken by SO_2 to form sulfate has major implications for both the radiative effects and the environment— in gas-phase reactions occurring predominantly with hydroxyl radicals (OH), the end-product sulfuric acid (g) leads to new particle formations eventually altering the cloud albedo and lifetime[4]. In the heterogenous phase reactions occurring primarily in cloud droplets via several oxidants, the major ones being O_2+TMI (Transition Metal Ion), H_2O_2, O_3 and NO_2, the end-product sulfate particles contribute towards modifying the aerosol size distribution and cloud condensation nuclei activity[5]. On a global scale, the sulfate aerosols contribute to a negative effective radiative forcing (ERF) of -0.90 (-0.24 to -1.56) W m^{-2} (IPCC, 2021). As such, the net cooling effect of sulfate aerosols partially counteracts the warming effects of greenhouse gases (e.g., CO_2, CH_4)[3,6]. However, the magnitude and expected future changes in sulfate aerosol radiative forcing remains one of the largest uncertainties associated with assessments of climate change[6].

To this end, S-isotope geochemistry can be used towards addressing these uncertainties as it provides powerful information for deconvolution of both emission sources and atmospheric processes[7-9]. Sulfur has four stable isotopes, ^{32}S, ^{33}S, ^{34}S and ^{36}S whose natural abundances are approximately 95%, 0.75%, 4.2% and 0.015%, respectively[10,11]. The S-stable isotopes undergo fractionation during kinetic and equilibrium reactions which causes the reactant (SO_2) and the

product (sulfate) to have distinct isotope compositions[12,13]. In general, the isotope ratios of any two isotopes can be scaled to each other based on the mass i.e., "mass dependent fractionation (MDF)" model[9]. More specifically, the fractionation factors determined for MDF processes follow a relation $^{3y}a=(^{34}a)^{3y_b}$ wherein ^{3y}a could be ^{33}a or ^{36}a and ^{3y}b is ^{33}b or ^{36}b and the 3yb is the relative fractionation of $^{3y}S/^{32}S$ and $^{34}S/^{32}S$[13]. The ^{33}b and ^{36}b values were experimentally determined to be 0.515 and 1.889[14]. Any deviation from this relationship implies the occurrence of "Mass Independent Fractionation (MIF)"[15]. The S-MIF is expressed as $\Delta^{33}S = (\delta^{33}S+1) - (\delta^{34}S+1)^{0.515}$ and $\Delta^{36}S = (\delta^{36}S+1) - (\delta^{34}S+1)^{1.889}$. Considerable debate exists in the interpretation of S-MIF signals observed in atmospheric aerosols from urban locations[e.g.,16-18].

The origin of S-MIF in nature has been primarily attributed to photochemical reactions in the presence of UV radiation —SO_2 absorption at 190-220 nm i.e., photolysis, and SO_2 absorption at 250-330 nm i.e., photo-oxidation[15]. These mechanisms have been suggested to account for the S-MIF observed in the Archean sediments as well as in modern aerosols[15,17]. However, to date the reported S-MIF values ranging from -0.6‰ to +0.6‰ evidenced in urban aerosols from polluted regions (e.g., Beijing, Montreal; Supporting Information (SI) Figure S1) have not been fully explicable with the S-isotope variations in emission sources (e.g., biomass or fossil fuel combustion with $\Delta^{33}S$ upto ~ ±0.2%) or atmospheric oxidation processes (e.g., homogenous and heterogenous reactions displaying $\Delta^{33}S \sim 0\%$)[16-18]. While a stratospheric origin of sulfate aerosols has been conceived to perpetuate $\Delta^{33}S$ in urban aerosols[17], this is not the case for all locations and cannot fully resolve the signals reported worldwide[16]. Taken together, this invokes the necessity for additional oxidation pathways or reactions to be identified for the conversion of SO_2 to sulfate affecting the $\Delta^{33}S$ in atmospheric aerosols[16]. As such, it could be a contributing factor for the uncertainties associated with the radiative forcing of sulfate aerosols on a global scale, and

especially in one of the most polluted regions of the world with rising SO_2 levels i.e., S Asia[19]. We therefore conducted dual-isotope fingerprinting ($\Delta^{33}S$, $\delta^{34}S$) of ambient sulfate aerosols in summertime megacity Delhi in S Asia. Combining chemical, isotopic, and meteorological information enabled resolving the origin of S-MIF anomalies in one of the most polluted regions in the world.

MATERIALS AND METHODS

Sampling. Aerosol PM_{10} samples (n=44) were collected using an Envirotech Air Pollution Monitoring 550 aerosol sampler, operated at 1 m^3 hr^{-1} with a sampling duration of 24 hours (sample collection started at 6 am and continued till 6 am of the next day; see SI Table S1). Sample collection was made between April-May 2021 atop a five-storey residential building in the Anand Vihar area of Delhi. The area is surrounded by parks and greenery. The sampling period covers the summer season. Delhi has a semi-arid climate and summer temperatures are on average 45±3 °C[20]. Aerosol samples were collected on pre-combusted (450 °C for 6 h) PALLFLEX tissue quartz filters (25 cm×20 cm). Filter blanks were collected approximately three times per month. Samples were stored in a freezer at −20 °C prior to analysis.

Chemical and Isotope Measurements. The concentration of water-soluble ions and metals, as well as the S-isotope compositions were measured using an ion chromatography Metrohm IC (Professional 850) and QQQ-ICP-MS, and a MC-ICP-MS instrument respectively. Measurements were carried out at the University of Tours (for water-soluble ions) and Centre de Recherches Pétrographiques et Géochimiques, CRPG (for S-isotopes) in France, and the Université du Québec à Montréal, UQAM (for metals) in Canada, respectively. Further details on the procedure,

measurements, analytical uncertainties, quality control and reproducibility are provided in SI Note S1.

RESULTS AND DISCUSSION

Summertime aerosol characteristics and multi-S-isotope compositions in S Asia. The megacity Delhi—located in the heart of the Indo-Gangetic Plain—suffers from acute air pollution crisis[20]. High average PM_{10} concentrations were found during the study period, 90±30 μg/m^3 in the months of April and 200±80 μg/m^3 in May 2021 (SI Table SI). This is attributable in general to features such as several types of anthropogenic activities, collocated emission sources, location and topography, population density, and socio-economic development[20-22]. Furthermore, long-range transport of dust from the adjoining Thar Desert and Arabian regions is also known to contribute towards episodic dust storms and high PM levels during summer[20].

The water-soluble inorganic ions (e.g., SO_4^{2-}, K^+) together contributing as much as 50% to the PM_{10} concentrations serve as tracers for combustion sources and secondary formation processes[20-23]. Concentrations of one such component, aerosol sulfate, ranged from 1 to 23 μg/m^3 (Figure 1a) implying a fractional contribution of upto 20% in the PM_{10} aerosols. The multi-S isotope compositions from Delhi ranged from 0.5‰ to 5‰ for $\delta^{34}S$, from 0.2‰ to 0.5‰ for $\Delta^{33}S$ during summer of 2021 (SI Table S2). In contrast to the observations of low $\Delta^{33}S$ (< 0.1‰) in the city of Montreal and high $\Delta^{33}S$ (~0.5‰) in its corresponding sub-rural background[16], here we find such higher values in the city. This however is in accordance with the finding from Beijing (i.e., E Asia) where a gradient shifting from ~0‰ to positive $\Delta^{33}S$ values (~0.5‰) has been reported during the summer[16,17,23]. For $\delta^{34}S$, the values are in general lower than those reported for Montreal

and Beijing during summer[16, 23], with values lower than 1‰ also being encountered in Delhi during the latter part of the summer. A shift towards concomitantly high $\Delta^{33}S$ and low $\delta^{34}S$ values was observed with proceeding of the summer season (Figure 1a) and could be driven by change in the sources and/or atmospheric processes.

Evaluation of plausible factors contributing to the sulfate $\Delta^{33}S$ dynamics. The measurements of multiple S-isotope composition reported here constitute the first for S Asia. The span of the $\Delta^{33}S$ values in the present study is such that it cannot be explained by the model proposed by Harris et al. (2013). Their model, relying upon the seasonal isotope variations induced by three major oxidation pathways (OH, H_2O_2, O_2+TMI), accounts for a maximum $\Delta^{33}S$-value of 0.05‰ during summer[18]. This implies that the additional $\Delta^{33}S$ dynamics observed in summertime Delhi could either be linked to changes in origin and/or possibly other chemical reactions.

The anthropogenic emission sources could modulate the $\Delta^{33}S$ values[17,23,24]. In particular, biomass burning and/or biofuel combustion have been shown to affect the urban $\Delta^{33}S$ signatures[23]. However, for the summer samples, a poor correlation was found between $\Delta^{33}S$ and K^+ (a tracer for biomass burning) (SI Figure S2). Coal combustion was found to be a large source of aerosol sulfate in Delhi based on source-apportionment using $\delta^{34}S$ (see SI Note S2), however, lab-based studies have shown both SO_2 and sulfate formed from coal combustion do not carry any $\Delta^{33}S$[17]. Iron extraction from Archean banded-iron formation (BIF) is another source of atmospheric S that produces non-zero $\Delta^{33}S$[16]. However, no such activities exist in and around the city[20,21]. Taken together this suggests that anthropogenic activities do not cause the observed $\Delta^{33}S$ isotope anomalies.

Stratospheric intrusions have been implicated for the $\Delta^{33}S$ observed in urban aerosols[17]. However, HYSPLIT model-based back trajectories do not show air masses arriving from the upper

troposphere (> 10-15 km) to the sampling location (SI Figure S3). This is consistent with the study of Lin et al. (2016) who also estimated a very low (< 1%) input of stratospheric SO_4 in their study[25]. Even with such an input only upto +0.1‰ of the $\Delta^{33}S$ anomaly may be explained, but not the entire range witnessed here. Furthermore, such intrusions are more common during the monsoon season than during the summer season in the Indian sub-continent[26] , which is further corroborated by the low cloud optical thickness and high cloud top pressure measurements during the summer of 2021 at Delhi (SI Figure S4). We therefore turn our attention to the possibility of chemical reactions/ mechanisms in order to explain the origin of the $\Delta^{33}S$ values observed in our sulfate aerosols.

Linking chemical and dual S-isotope signals to deconvolute sulfate formation. Recently, the role of mineral dust in the formation of secondary aerosol sulfate has been called into contention[16]. The mechanisms behind the formation of secondary aerosol sulfate mediated by mineral dust remain elusive[16,27]. For instance, they may include oxidation of SO_2 by the superoxide radical anion formed on semi-conducting metal oxides like Al_2O_3, Fe_2O_3 and TiO_2 by UV radiation, oxidation by NO_2[16]. Interestingly, our chemical analyses indicate significant contributions of mineral dust in the PM_{10} aerosols in Delhi as samples present Fe/Al ratios (i.e., the conventional reference for upper continental crust)[28,29] from as low as 0.2 during April to as high as 1.4 during May (all > 0.05; Figure 1a), similar to the ones characterizing desert dusts (from 0.48 to 1.74)[29]. We elected to discuss the Fe/Al ratio which is more representative of mineral dust than the Ca^{2+}/Al ratio, mainly a tracer for carbonate mineral[28,29].

Higher Fe/Al ratios were observed with the progression of the summer season concomitant with the influx of mineral dust from the Thar desert in western India, as evidenced by air mass analysis and satellite data (SI Figures S3, S5). We find strong correlations between the Fe/Al ratios and the sulfate loadings (R^2=0.84) and $\Delta^{33}S$ values (R^2=0.77) respectively, highlighting a potential

link between the sulfate formation, S-isotope variations and mechanisms involving mineral dust. In fact, the higher $\Delta^{33}S$ anomalies (> 0.2‰) observed in the month of May were concomitant with 5-times higher loadings of mineral dust relative to those of April 2021. Taken together, this implies that the low $\Delta^{33}S$ values (< 0.2‰) are indeed not greatly affected by mineral dust contribution and can be explained as arising from a combination of different sources/origins and other homogenous and heterogenous oxidation pathways (upto ~ +0.20‰) or even stratospheric intrusions[17,18,23]. But the higher $\Delta^{33}S$ values (as well as sulfate concentrations) observed in Delhi during summer of 2021 were strongly modulated by the presence of mineral dust.

Weak winds combined with a shallow boundary layer can lead to the contribution of high fine mode resuspended road dust (whose composition remains unknown). This has been observed in E Asia during the haze episodes[30]. However, such meteorological conditions are more favourable for wintertime S Asia than summer[20,22]. The terrigenous sulfate source fraction ($f_{ter\text{-}S}$) is useful for accounting the contribution of local resuspended dust (from within the city). Here, based on ratio of SO_4^{2-}-to-Ca^{2+} concentrations in regional soil to the same in sampled aerosol, we accounted for the $f_{ter\text{-}S}$ in summertime Delhi samples (Figure 1c; see also Note S2). We find that the $f_{ter\text{-}S}$ decreased from 20±5% on average in April to <5±2% during May of 2021. This decrease in $f_{ter\text{-}S}$ is concomitant with the increase in the Fe-to-Al ratio. This implies that influx of mineral dust from nearby desert region in W India modulated the formation of aerosol sulfate and thereby the observed high $\Delta^{33}S$ values (as desert dust carries no S-MIF)[16] as the summer progressed. This also points to the fact that the $\delta^{34}S$ signature of mineral dust from the Thar desert might be slightly lower than that from deserts in China, Morocco, Tunisia and Jordan, with $\delta^{34}S$ ranges between 5 and 13‰[16].

Implications of mineral dust on sulfate-induced urban air pollution. Overall, the present findings suggest that $\Delta^{33}S$ is a reliable tracer for better constraining the formation of sulfate aerosols in the presence of mineral dust. Comparing with previous observations from a sub-rural background site in Montreal (referred to as station 98 in Au Yang et al., 2019), we find overlapping characterisitcs in both $\Delta^{33}S$ and $\delta^{34}S$ (Figure 2). Here, we conjecture that the high $\Delta^{33}S$ values recorded at station 98 are indeed explicable by the SO_2 photo-oxidation on mineral dust pathway in line with the hypothesis by Au Yang et al. . Furthermore, with an estimated $\Delta^{33}S$ fingerprint of +0.35±0.10‰ for this pathway, we are able to also explain the $\Delta^{33}S$ values previously observed in other urban locations such as in E Asia (Figure 2) hinting at a plausible global significance of this pathway. The implications of the findings here are twofold (i) even a small contribution from mineral dust-mediated SO_2 photo-oxidation may have a large effect on the observed $\Delta^{33}S$ signals in aerosols, (ii) regions with low SO_2 production but high input of mineral dust e.g., remote oceanic regions[22], can still act as emission regions of sulfate aerosols, thereby affecting the aerosol radiative forcing. It remains to be seen if this pathway sustains during vertical transport of SO_2 where competing mechanisms such as aqueous phase oxidation and/or stratospheric intrusions become more relevant[31].

For South Asia, the rising SO_2 levels present a threat to several of the sustainable development goals for the region such as access to clean air and freshwater[32,33]. For accurate predictions of future scenarios of the influence of SO_2 on the region it is imperative to account for all sources and formation pathways of sulfate. We therefore consider that the findings here would aid in that direction and contribute towards reducing the model-observation discrepancies in modeling global and regional sulfate aerosol dynamics wherein the sensitivity of the simulations remains highly dependent on the accounted oxidation pathways[34].

FIGURES

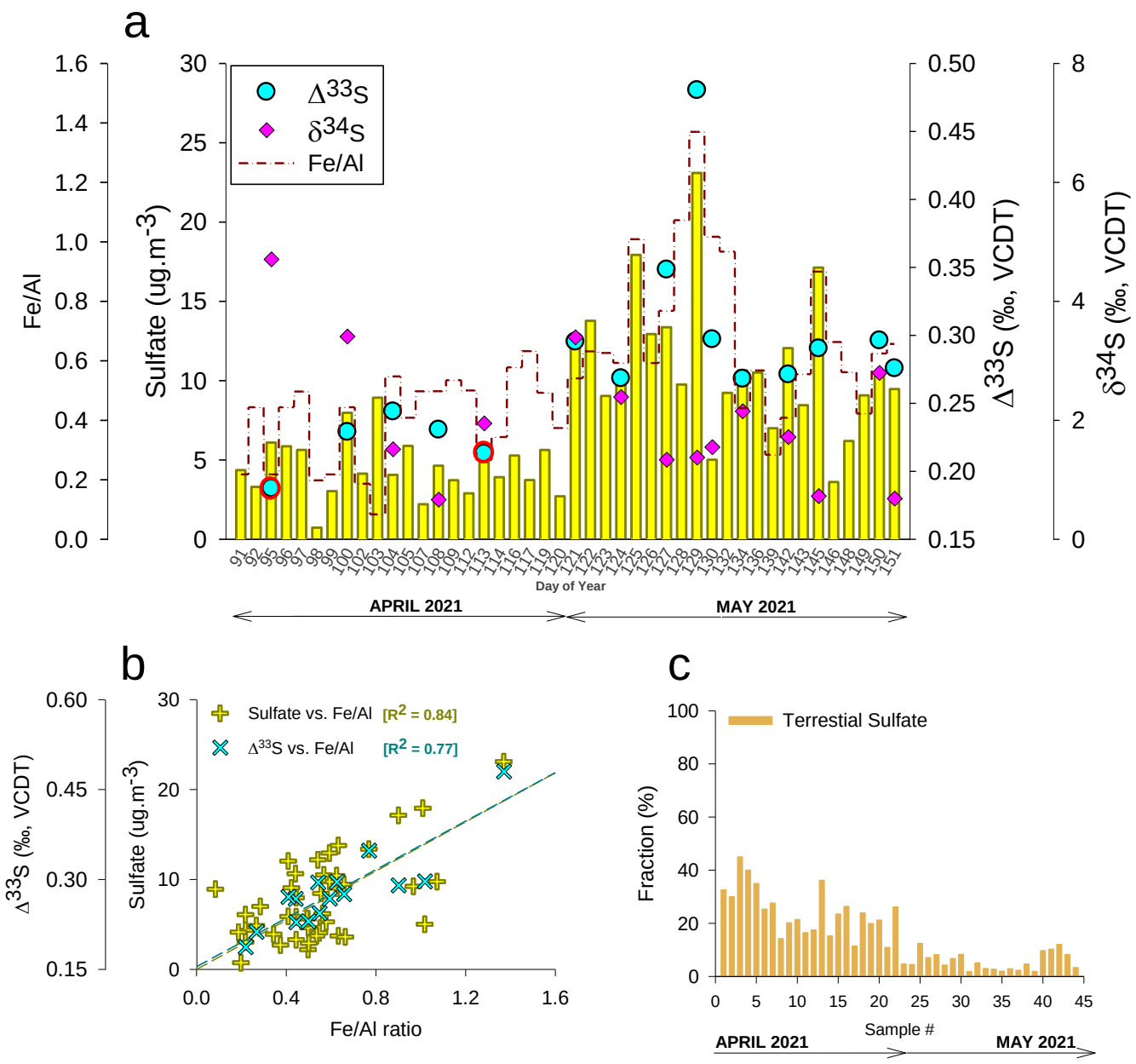

Figure 1. (A) Temporal changes in the sulfate concentrations, $\Delta^{33}S$, $\delta^{34}S$ and Fe/Al ratios, (B) Correlation of the $\Delta^{33}S$ signals, sulfate loadings with the influx of mineral dust (see also, SI Table S1-S2, SI Figures S3-S5), (C) Calculated terrestrial sulfate fraction in the PM_{10} samples (see

also SI Note S2). Samples with red circles (Day 95, 113) refer to the ones collected only during the nighttime (6 pm to 6 am). As such, these were restricted to 12 h collections.

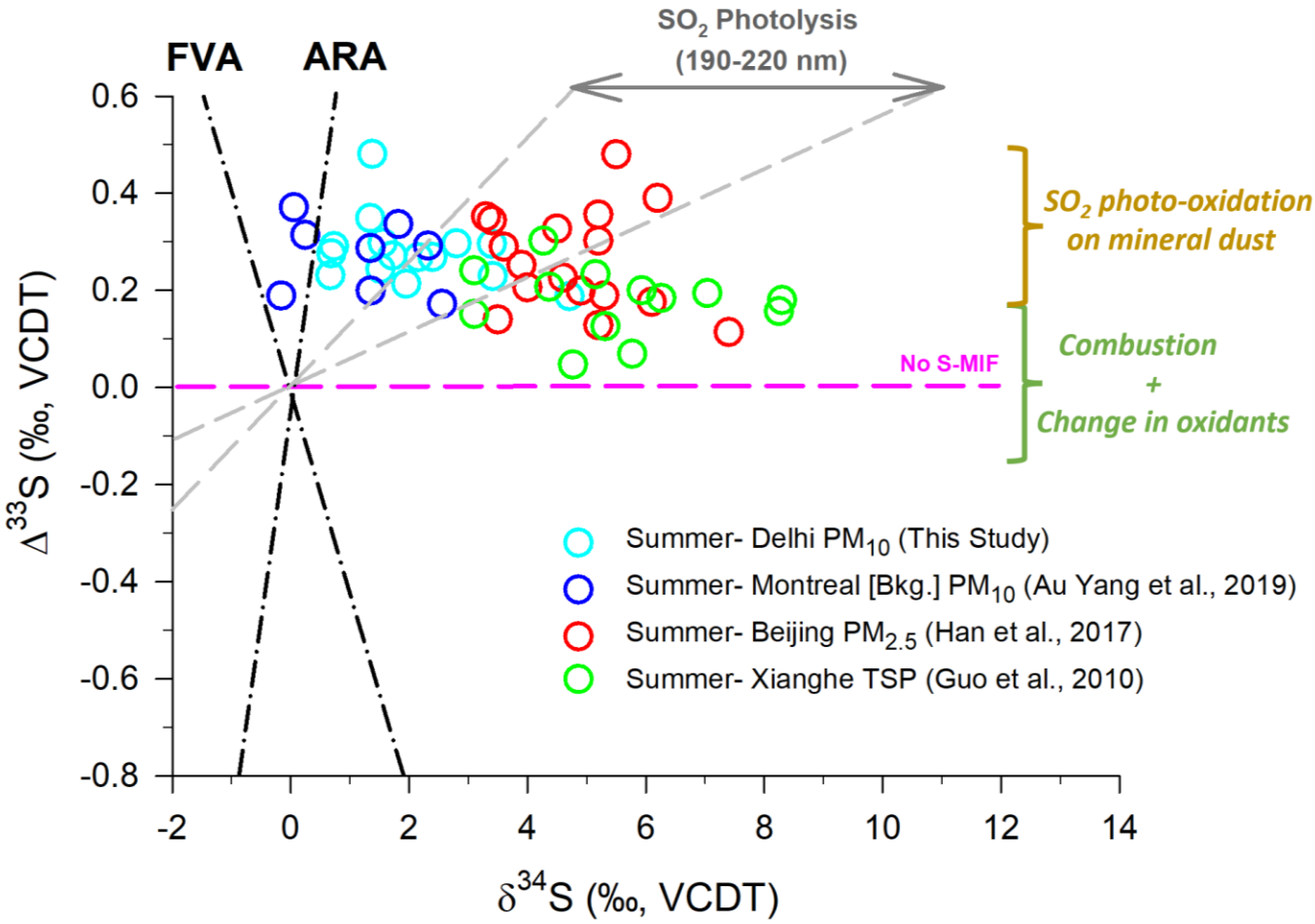

224

225

226 **Figure 2.** Relation between $\Delta^{33}S$ and $\delta^{34}S$ for sulfate in Delhi PM_{10} during sampling and their
227 comparison with aerosols collected from Beijing[23] and Xianghe in E Asia[35] and sub-rural
228 background site in Montreal, Canada[16]. ARA represents the Archean Reference Array based on
229 the data from Neoarchean and Paleoarchean rocks in Australia and Africa[36]. FVA represents the
230 felsic volcanic array[37]. The gray field represents experiment data from SO_2 photolysis in the
231 190−220 nm region (Xenon arc lamp)[15].

ASSOCIATED CONTENT

Supporting Information. Notes S1-S2 include discussions on the chemical and isotope measurements, source apportionment calculations. Figures S1-S5 include air mass analysis, satellite data-derived maps, correlations. Tables S1-S2 list the sampling details and concentrations of water-soluble ions, metals, and multiple S-isotope compositions.

AUTHOR INFORMATION

Corresponding Authors

* E-mail: sanjeev.dasari@univ-grenoble-alpes.fr ; widory.david@uqam.ca

Phone: +33 068 564 42 84 ; +1 438 998 11 13

Author Contributions

S.D. designed research and was supported by D.W., Z.C and G.P.; S.D., B.S., and G.P performed the chemical and isotopic measurements, respectively; All co-authors analyzed data; S.D., wrote the paper with input from all co-authors.

Funding Sources

This work was supported by the French National CNRS-INSU program LEFE (Les Enveloppes Fluides et l'Environnement; grant awarded to G.P). D.W. and Z.C. acknowledge financial support from the Université du Québec à Montréal and the Chinese Academy of Sciences, respectively.

Notes

The authors declare no competing financial interests.

ACKNOWLEDGMENTS

Pavan Datta is acknowledged for organization and on-field support with filter sampling in Delhi, India. Nathalie Gassama at the University of Tours, France is acknowledged for support with IC analysis.

REFERENCES

1. Thode, H. G. Sulphur isotopes in nature and the environment: an overview. *Stable isotopes: natural and anthropogenic sulphur in the environment* **1991**, *43*, 1-26 https://scope.dge.carnegiescience.edu/SCOPE_43/SCOPE_43_1_Chp1.pdf (accessed 2021.12).

2. Seinfeld, J. H.; Pandis, S. N. *Atmospheric Chemistry and Physics: From Air Pollution to Climate Change*; John Wiley & Sons, 2016.

3. *Climate change 2007: The Physical Science basis; https://www.ipcc.ch/report/ar4/wg1/ , 2007.*

4. Kulmala, M.; Riipinen, I.; Sipilä, M.; Manninen, H. E.; Petäjä, T.; Junninen, H.; Dal Maso, M.; Mordas, G.; Mirme, A.; Vana, M.; Hirsikko, A. Toward direct measurement of atmospheric nucleation. *Science* **2007**, *318*, 89-92.

5. Mertes, S.; Galgon, D.; Schwirn, K.; Nowak, A.; Lehmann, K.; Massling, A.; Wiedensohler, A.; Wieprecht, W. Evolution of particle concentration and size distribution observed upwind, inside and downwind hill cap clouds at connected flow conditions during FEBUKO. *Atmos. Environ*. **2005**, *39*, 4233−4245.

6. Arias, P.; Bellouin, N.; Coppola, E.; Jones, R.; Krinner, G.; Marotzke, J.; Naik, V.; Palmer, M.; Plattner, G. K.; Rogelj, J.; Rojas, M. Climate Change 2021: The Physical Science Basis. Contribution of Working Group14 I to the Sixth Assessment Report of the Intergovernmental Panel on Climate Change; Technical Summary **2021**.

7. Nriagu, J. O.; Coker, R. D.; Barrie, L. A. Origin of sulphur in Canadian Arctic haze from isotope measurements. *Nature* **1991**, *349*, 142-145.

8. Shen, Y.; Buick, R.; Canfield, D. E. Isotopic evidence for microbial sulphate reduction in the early Archaean era. *Nature* **2001**, *410*, 77–81.

9. Farquhar, J.; Bao, H.; Thiemens, M. Atmospheric influence of Earth's earliest sulfur cycle. *Science* **2000**, *289*, 756-758.

10. Ding, T.; Valkiers, S.; Kipphardt, H.; De Bievre, P.; Taylor, P.; Gonfiantini, R.; Krouse, R. Calibrated sulfur isotope abundance ratios of three IAEA sulfur isotope reference materials and V-CDT with a reassessment of the atomic weight of sulfur. *Geochim. Cosmochim. Acta* **2001**, *65*, 2433–2437.

11. Coplen, T. B. Guidelines and recommended terms for expression of stable-isotope-ratio and gas-ratio measurement results. *Rapid Comm. Mass Spec*. **2011**, *25*, 2538–2560.

12. Ono, S.; Wing, B.; Johnston, D.; Farquhar, J.; Rumble, D. Mass-dependent fractionation of quadruple stable sulfur isotope system as a new tracer of sulfur biogeochemical cycles, *Geochim. Cosmochim. Acta* **2006**, *70*, 2238–2252.

13. Dauphas, N.; Schauble, E. A. Mass fractionation laws, mass independent effects, and isotopic anomalies. *Ann. Rev. Earth Pl. Sci*. **2016**, *44*, 709–783.

14. Eldridge, D.; Guo, W.; Farquhar, J. Theoretical estimates of equilibrium sulfur isotope effects in aqueous sulfur systems: Highlighting the role of isomers in the sulfite and sulfoxylate systems. *Geochim. Cosmochim. Acta* **2016**, *195*, 171–200.

15. Whitehill, A. R.; Jiang, B.; Guo, H.; Ono, S. SO_2 photolysis as a source for sulfur mass-independent isotope signatures in stratospheric aerosols. *Atmos. Chem. Phys*. **2015**, *15*, 1843-1864.

16. Au Yang, D.; Cartigny, P.; Desboeufs, K.; Widory, D. Seasonality in the $\Delta^{33}S$ measured in urban aerosols highlights an additional oxidation pathway for atmospheric SO_2. *Atmos. Chem. Phys*. **2019**, *19*, 3779-3796.

17. Lin, M.; Zhang, X.; Li, M.; Xu, Y.; Zhang, Z.; Tao, J.; Su, B.; Liu, L.; Shen, Y.; Thiemens, M. H. Five-S-isotope evidence of two distinct mass-independent sulfur isotope effects and implications for the modern and Archean atmospheres. *Proc. Natl. Acad. Sci. U. S. A*. **2018**, *115*, 8541-8546.

18. Harris, E.; Sinha, B.; Hoppe, P.; Ono, S. High-precision measurements of ^{33}S and ^{34}S fractionation during SO_2 oxidation reveal causes of seasonality in SO_2 and sulfate isotopic composition. *Environ. Sci. Technol.* **2013**, *47*, 12174–12183.

19. Dahiya, S.; Myllyvirta, L. Global SO_2 Emission Hotspots Database: Ranking the World'S Worst Sources of SO_2 Pollution. Greenpeace Environment Trust, https://www.greenpeace.org/india/en/publication/3951/global-so2-emission-hotspots-database-ranking-the-worlds-worst-sources-of-so2-pollution-2/(accessed 2021.12)

20. Hama, S. M.; Kumar, P.; Harrison, R. M.; Bloss, W. J.; Khare, M.; Mishra, S.; Namdeo, A.; Sokhi, R.; Goodman, P.; Sharma, C. Four-year assessment of ambient particulate matter and trace gases in the Delhi-NCR region of India. *Sustain. Cit. Soci.* **2020**, *54*, 102003.

21. Gurjar, B. R.; Nagpure, A. S. Indian megacities as localities of environmental vulnerability from air quality perspective. *J. Smart Cities* **2016**, *1*,15-30.

22. Dasari, S.; Andersson, A.; Bikkina, S.; Holmstrand, H.; Budhavant, K.; Satheesh, S.; Asmi, E.; Kesti, J.; Backman, J.; Salam, A.; Bisht, D. S. Photochemical degradation affects the light absorption of water-soluble brown carbon in the South Asian outflow. *Sci. Adv.* **2019**, 5, eaau8066.

23. Han, X.; Guo, Q.; Strauss, H.; Liu, C.; Hu, J.; Guo, Z.; Wei, R.; Peters, M.; Tian, L.; Kong, J. Multiple sulfur isotope constraints on sources and formation processes of sulfate in Beijing PM2:5 aerosol. *Environ. Sci. Technol*. **2017**, *51*, 7794–7803.

24. Lee, C. W.; Savarino, J.; Cachier, H.; Thiemens, M. Sulfur (^{32}S, ^{33}S, ^{34}S, ^{36}S) and oxygen (^{16}O, ^{17}O, ^{18}O) isotopic ratios of primary sulfate produced from combustion processes. *Tellus B* **2002**, *54*, 193–200.

25. Lin, M.; Zhang, Z.; Su, L.; Hill-Falkenthal, J.; Priyadarshi, A.; Zhang, Q.; Zhang, G.; Kang, S.; Chan, C. Y.; Thiemens, M. H. Resolving the impact of stratosphere-to-troposphere transport on the sulfur cycle and surface ozone over the Tibetan Plateau using a cosmogenic 35S tracer. *J. Geophys. Res. Atmos.* **2016**, *121*, 439–456.

26. Fadnavis, S.; Chattopadhyay, R. Linkages of subtropical stratospheric intraseasonal intrusions with Indian summer monsoon deficit rainfall. *J. of Climate* **2017**, *30*, 5083-5095.

27. Harris, E.; Sinha, B.; Foley, S.; Crowley, J. N.; Borrmann, S.; Hoppe, P. Sulfur isotope fractionation during heterogeneous oxidation of SO_2 on mineral dust. *Atmos. Chem. Phys*. **2012**, *12*, 4867– 4884.

28. Paris, R.; Desboeufs, K. V.; Formenti, P.; Nava, S.; Chou, C. Chemical characterisation of iron in dust and biomass burning aerosols during AMMA-SOP0/DABEX: implication for iron solubility. *Atmos. Chem. Phys*. **2010**, *10*, 4273–4282.

29. Formenti, P.; Schütz, L.; Balkanski, Y.; Desboeufs, K.; Ebert, M.; Kandler, K.; Petzold, A.; Scheuvens, D.; Weinbruch, S.; Zhang, D. Recent progress in understanding physical and chemical properties of African and Asian mineral dust. *Atmos. Chem. Phys*. **2011**, *11*, 8231–8256.

30. Tian, S. L.; Pan, Y. P.; Wang, Y. S. Size-resolved source apportionment of particulate matter in urban Beijing during haze and non-haze episodes. *Atmos. Chem. Phys*. **2016**, *16*, 1-19.

31. Lin, M.; Biglari, S.; Zhang, Z.; Crocker, D.; Tao, J.; Su, B.; Liu, L.; Thiemens, M. H. Vertically uniform formation pathways of tropospheric sulfate aerosols in East China detected from triple stable oxygen and radiogenic sulfur isotopes. *Geophys. Res. Lett*. **2017**, *44*, 5187-5196.

32. Fadnavis, S.; Müller, R.; Kalita, G.; Rowlinson, M.; Rap, A.; Li, J. L. F.; Gasparini, B.; Laakso, A. The impact of recent changes in Asian anthropogenic emissions of SO_2 on sulfate loading in the upper troposphere and lower stratosphere and the associated radiative changes. *Atmos. Chem. Phys.* **2019**, *19*, 9989-10008.

33. Fadnavis, S.; Sabin, T. P.; Roy, C.; Rowlinson, M.; Rap, A.; Vernier, J. P.; Sioris, C. E. Elevated aerosol layer over South Asia worsens the Indian droughts. *Sci. Rep*. **2019**, *9*, 1-11.

34. Paulot, F.; Paynter, D.; Ginoux, P.; Naik, V.; Horowitz, L.W. Changes in the aerosol direct radiative forcing from 2001 to 2015: observational constraints and regional mechanisms. *Atmos. Chem. Phys*. **2018**, *18*, 13265-13281.

35. Guo, Z.; Li, Z.; Farquhar, J.; Kaufman, A. J.; Wu, N.; Li, C.; Dickerson, R. R.; Wang, P. Identification of sources and formation processes of atmospheric sulfate by sulfur isotope and scanning electron microscope measurements. *J. of Geophys. Res. Atmos*. **2010**, *115*, D00K07.

36. Mast, M. A.; Turk, J. T.; Ingersoll, G. P.; Clow, D. W.; Kester, C. L. Use of stable sulfur isotopes to identify sources of sulfate in Rocky Mountain snowpacks. *Atmos. Environ.* **2001**, *35*, 3303−3313.

37. Philippot, P.; van Zuilen, M.; Rollion-Bard, C. Variations in atmospheric sulphur chemistry on early Earth linked to volcanic activity. *Nat. Geosci*. **2012**, *5*, 668−674.

369 **TOC GRAPHICAL ABSTRACT**